ChemComm

Functional Polymers for Growth and Stabilization CsPbBr3 Perovskite Nanoparticles

Journal:	*ChemComm*
Manuscript ID	CC-COM-11-2018-009343.R1
Article Type:	Communication

Journal Name

COMMUNICATION

Functional Polymers for Growth and Stabilization of $CsPbBr_3$ Perovskite Nanoparticles

Hyunki Kim[a], Soonyong So[a,b], Alexander Ribbe[a], Yao Liu[a], Weiguo Hu[a], Volodimyr V. Duzhko[a], Ryan C. Hayward,[a,*] and Todd Emrick[a,*]

Received 00th January 20xx,
Accepted 00th January 20xx

DOI: 10.1039/x0xx00000x
www.rsc.org/

We introduce an approach to synthesize polymer-stabilized $CsPbBr_3$ perovskite nanoparticles (NPs) using ammonium bromide-functionalized polymers as both bromide precursors and stabilizing ligands. The polymer-passivated NPs exhibit significant advantages over conventional perovskite NPs owing to their facile dispersion in polymer matrices and enhanced optoelectronic stability.

Perovskites with the structural formula AMX_3 (A = cation, M = metal, and X = halide) are advancing rapidly in electronic materials science.[1] Owing to their crystallinity, strong optical absorption, small exciton binding energy, balanced electron-hole mobility, and long exciton diffusion lengths,[2-4] perovskite solar cells have exceeded 20% power conversion efficiency (PCE) in photovoltaic devices.[5] Furthermore, halide-containing perovskite nanoparticles (NPs) promote exciton recombination and exhibit tunable bandgaps, providing potential benefits to light-emitting diodes (LEDs),[6] lasers,[7] and two-photon absorbers.[8]

The synthesis of colloidal $CH_3NH_3PbBr_3$ perovskite NPs from precursor salts and surfactants in solution was reported by Pérez-Prieto and coworkers.[9] Kovalenko subsequently described a hot injection method to achieve all inorganic $CsPbX_3$ NPs with photoluminescence (PL) quantum yield (QY) up to 90%, narrow full-width at half-maximum (FWHM) emission, and tunable bandgap.[10] Unlike more conventional quantum dots, such as CdSe, these $CsPbX_3$ NPs did not require wide bandgap inorganic passivating shells to achieve high QY, due to a high tolerance for defects.[11] Furthermore, the FWHM of PL emission from $CsPbBr_3$ NPs is relatively insensitive to NP size distribution, which is beneficial for devices that require color purity.[12]

A serious problem associated with halide-containing perovskites is their sensitivity to humidity and air. For example, moisture causes bulk $CH_3NH_3PbI_3$ to decompose and produce an additional PbI_2 phase.[13] This is exacerbated in perovskite NPs due to their high surface-to-volume ratios.[14] When $CsPbBr_3$ NPs were precipitated into polar solvents, their PL decreased significantly, followed by loss of colloidal stability.[15] To overcome these issues, Li and coworkers developed silica-passivated perovskite NPs,[14] while interdigitation of the alkyl chains of NP ligands with alkyl-substituted polymers or a nanocomposite of the NPs with poly(styrene-ethylene-butylene-styrene) was shown to improve perovskite NP stability.[16, 17] Another recent report described the synthesis of $CsPbBr_3$ NPs in poly(styrene-*block*-(2-vinyl)pyridine) micelles to enhance NP stability.[18]

Here we report the synthesis of $CsPbBr_3$ perovskite NPs with ammonium bromide-containing polymers that serve as both stabilizing ligands and bromide precursors. Cube-shaped $CsPbBr_3$ NPs were generated following high temperature injection of the ammonium bromide-functionalized polystyrene into a metal-carboxylate precursor solution. This yielded polymer-passivated $CsPbBr_3$ NPs amenable to purification in non-polar solvents with retention of high photoluminescence quantum yield. In addition, polymer-passivated NPs produced optically clear nanocomposite films with enhanced stability over that of small molecule-passivated perovskite NPs. This strategy was then extended to $CsPbBr_3$ NPs stabilized by conjugated polymers for producing electronically active polymer-perovskite NP hybrid materials.

Ammonium bromide-terminated polystyrene was prepared and used for the preparation of perovskite NPs. The polymers were prepared by atom transfer radical polymerization (ATRP),[19] followed by Boc-deprotection to give the PS-NH_3Br. As it was recently reported that ammonium cations interact with surface bromides of $CsPbBr_3$ NPs by 'hydrogen bridging', or filling of octahedral holes on the perovskite surface,[15, 20] we surmised that such functional polymers would be ideal for stabilizing perovskite NP surfaces and acting as a source of bromide during NP growth. In typical experiments, Pb- and Cs-oleate (0.06 mmol) were dissolved in mesitylene (17 mL), a high boiling solvent useful for dissolving both metal oleates and ammonium bromide-containing polymers. The metal precursor solution was heated to 160 °C and ammonium bromide-functionalized polymers (2 g in 4 mL of mesitylene) were injected, producing the PS-ω-NH_3Br-passivated $CsPbBr_3$ NPs (PS-ω-NH_3Br

[a] Polymer Science & Engineering Department, University of Massachusetts, Amherst, MA 01003, United States. [b]Membrane Research Center, Korea Research Institute of Chemical Technology, Daejeon 34114, South Korea, †Electronic Supplementary Information (ESI) available: detailed synthesis procedure and characterizations (^{1}H NMR, UV/Vis and PL). See DOI: 10.1039/x0xx00000x

NPs). The resultant NPs were precipitated in hexane and redispersed in toluene. The preparation of the $CsPbBr_3$ NPs using a random copolymer of polystyrene and 2-methacryloyloxyethyl ammonium bromide is also described in the SI.

The PS-NH_3Br NPs exhibited high quantum yield (QY, 79%) and FWHM as narrow as 17 nm (**Figure 1A**). Powder X-ray diffraction (XRD, **Figure 1E**) experiments performed on the $CsPbBr_3$ NPs revealed a pattern consistent with either a cubic or an orthorhombic crystal structure; as reported previously, the broad diffraction peaks resulting from the small crystallite sizes complicate distinction between these two structures.[12] TEM (**Figure 1D**) showed cube-shaped NPs with cube edge length of 11.2 ± 4.6 nm. The photoluminescence (PL) full-width at half-maximum (FWHM) was narrow, despite a high standard deviation of particle size. In these samples, since the average crystal diameter is larger than the Bohr diameter of bulk $CsPbBr_3$ (7 nm),[12] these NPs are in the weak confinement regime, leading to a relatively size-insensitive bandgap.

The coordination of polymer ligands to $CsPbBr_3$ NPs modifies their solution properties and allows purification in non-polar solvents without substantial loss of PL QY. **Figure 1B-C** shows that when PS-ω-NH_3Br NPs were precipitated into hexanes, then redispersed in toluene, the QY recovered to its initial value, even following two purification cycles. In contrast, $CsPbBr_3$ NPs prepared with oleylamine and oleic acid ligands (oleyl NPs) did not precipitate in hexane, and two purification cycles involving precipitation in acetone caused the QY to decrease to <50 % of its original value. Such purification difficulties, with an associated decrease in QY and/or degradation to elemental precursor material, has been notably problematic.[15, 21] The use of a nonpolar solvent to purify polymer-passivated NPs therefore represents a potentially attractive route for perovskite NP isolation and processing without loss of their desirable optoelectronic properties.

To better characterize NP surface passivation of these hybrid materials, diffusion-ordered nuclear magnetic resonance spectroscopy (DOSY) was employed. Since ligands on $CsPbBr_3$ perovskite NPs are dynamic, the diffusion coefficient reflects the average of bound and unbound states.[22] As shown in **Figure 1G**, the proton signals at 6.6 ppm in benzene-d^6 were characterized by DOSY, employing polymer samples prior to Boc deprotection. The attenuation plot derived from the DOSY NMR spectrum, shown in **Figure 1F**, revealed a diffusion coefficient of 7.0 x 10^{-11} m^2/s (R_H = 5.1 nm) for the polymer-functionalized NPs, and 1.6 x 10^{-10} m^2/s (R_H = 2.2 nm) without the NPs, the difference attributed to surface coordination of the polymer.

Potential optoelectronic and device applications of these polymer-perovskite composites would benefit from optical transparency.[23] When a toluene solution of the PS-ω-NH_3Br NPs was dropcast onto silicon or glass, optically clear nanocomposite films were obtained; this is in contrast to oleyl NPs in polystyrene (Mn : 6.4 kg/mol) that appeared opaque, as shown in **Figure 2A** (inset). Aggregation of the oleyl NPs would be anticipated from the poor compatibility between the ligands and the polymer matrix.[24] The

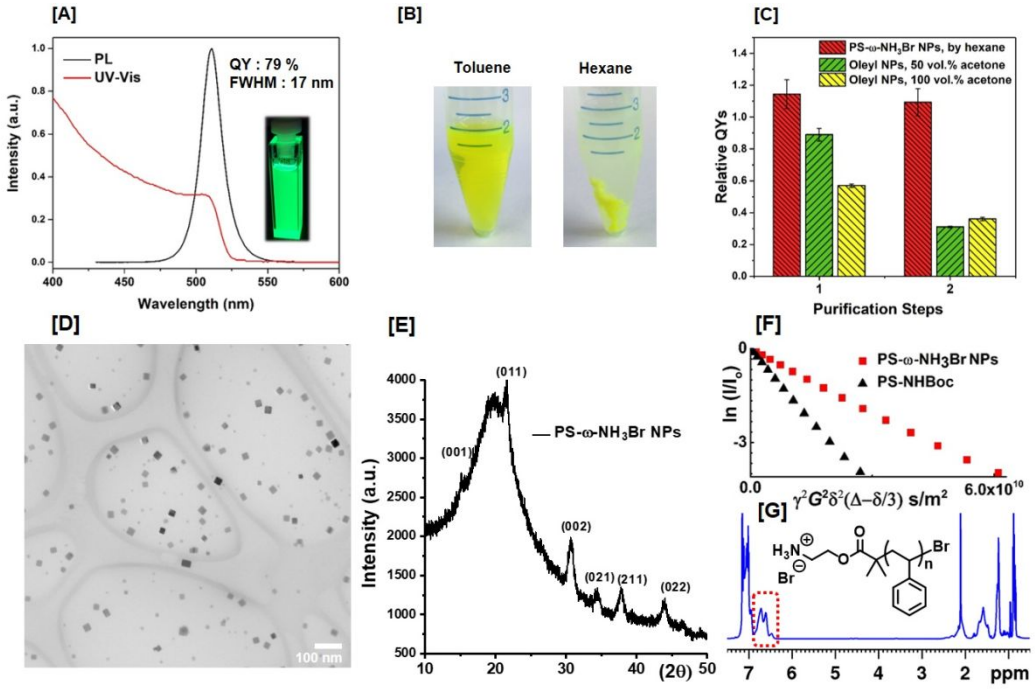

Figure 1. (A) UV-Vis and PL spectra of PS-ω-NH_3Br NPs; (B) Photograph of PS-ω-NH_3Br NPs in toluene (left) and hexane (right); (C) Relative PL QYs of $CsPbBr_3$ NPs with purification cycles using hexanes and acetone for PS-ω-NH_3Br NPs and oleyl NPs. The amount of the acetone added was 50 vol.% or 100 vol.% compared to the NP solution; (D) TEM image of the PS-ω-NH_3Br NPs; (E) XRD pattern of PS-NH_3Br NPs; (F) Attenuation plot derived from DOSY NMR spectroscopy in benzene-d^6, using the 6.6 ppm proton signals; on the x-axis, γ is proton gyromagnetic ratio, δ is the length of pulse sequence, G is the gradient strength and Δ is the diffusion time; (G) ^{1}H NMR spectrum of the PS-NH_3Br NPs (red box shows the spectral region used for DOSY analysis.)

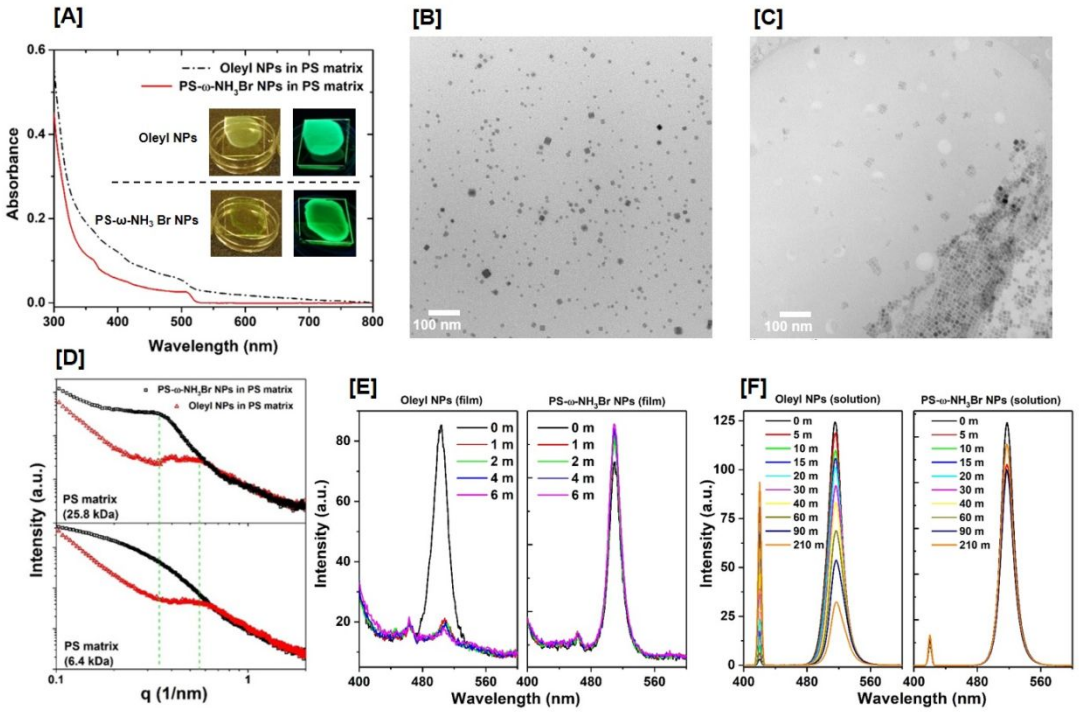

Figure 2. (A) UV-Vis spectra of PS-ω-NH_3Br NPs nanocomposite films; inset shows the PS-ω-NH_3Br NP film (bottom) and the oleyl NPs in the PS matrix (top) under no UV light (left) and with UV light (right); (B) TEM images of PS-ω-NH_3Br NPs in PS; (C) oleyl NPs in PS; (D) SAXS results for powders of PS-ω-NH_3Br NPs and the oleyl NPs in PS (M_n : 6.4 kg/mol and 25.8 kg/mol); (E) PL spectra of oleyl NPs (left) and the PS-ω-NH_3Br NPs (right) embedded in the PS thin film after immersion in 1-propanol (λ_{ex} = 360 nm); (F) PL spectra of colloidal oleyl NPs (left) and the PS-ω-NH_3Br NPs (right) in a toluene/1-propanol solvent mixture (2:1 volume fraction), (λ_{ex} = 420 nm).

representative TEM images in **Figure 2B-2C** confirm that the oleyl NPs aggregated considerably in polystyrene, whereas the PS-ω-NH_3Br NPs dispersed cleanly. To further confirm the aggregation/dispersion behavior of the nanocomposites, small-angle X-ray scattering (SAXS) measurements were performed on the nanocomposite powders. As shown in **Figure 2D**, the oleyl NPs in PS (Mn : 6.4 kg/mol) showed a characteristic d-spacing of 11.2 nm, consistent with the expected inter-particle spacing when the NPs packed closely (with edge length of 8.4 ± 1.4 nm and ligand shell thickness of 1.6 nm). PS-ω-NH_3Br NPs dispersed in the same polymer showed no such peak, due to the more diffuse and random NP dispersion in these samples. When the molecular weight of the PS matrix was increased to 25.8 kg/mol, PS-ω-NH_3Br NPs showed the characteristic peak with a d-spacing of 18.3 nm indicating some degree of NP aggregation (with edge length of 11.2 ± 4.6 nm and polymer ligand shell thickness ~ 7 nm), consistent with previous reports that NPs tend to aggregate when the molecular weight of polymers in the matrix exceeds that of the polymer ligands.[25]

The PS-ω-NH_3Br perovskite NPs also showed higher PL stability, relative to the oleyl NPs, in the presence polar solvents such as 1-propanol. As shown in **Figure 2E**, the PL intensity of spin-coated films containing oleyl NPs declined to about 12% of their initial value when immersed in 1-propanol for 1 minute. However, thin films containing the polymer-stabilized NPs did not show any degradation within 10 mins (**Figure S8**). Although the origin of this improved stabilization requires further study, we expect that the short alkyl chain-stabilized oleyl NPs may segregate to the air-polymer interface and be more readily exposed to the solvent, while the better-dispersed polymer-stabilized NPs are more effectively protected by the polymer matrix. In addition, as shown in **Figure 2F**, the polymer-stabilized NPs showed higher colloidal stability in toluene/1-propanol mixtures, possibly due to better local protection of NPs by polymer ligands in solution.

Having estabilished the stabilization of perovskite NPs with end-functionalized polymer ligands, we extended the concept to conjugated polymers. Ammonium bromide-terminated poly(9,9'-dioctylfluorene) (PF-NH_3Br) was synthesized by Suzuki-Miyaura coupling, employing a stoichiometric imbalance to favor a Boc group at one end (PF-NHBoc); subsequent Boc-deprotection yielded PF-NH_3Br (M_n = 3.9 kDa, Đ = 1.6, GPC against polystyrene standards with THF as eluent). The initial presence and subsequent loss of the Boc group were confirmed by MALDI-TOF mass spectrometry and ^1H NMR spectroscopy (**Figure 3A-B**) When PF-NH_3Br was used for NP synthesis, cube-shaped $CsPbBr_3$ NPs (PF-NH_3Br NPs) were obtained, as shown in the TEM of **Figure 3C**. The PL spectra of the resultant solution (**Figure 3D**) revealed the PF-NH_3Br NPs to have spectral features from both the conjugated polymer ligand and the $CsPbBr_3$ NP core. When PLE spectra were recorded with an emission peak at 510 nm, corresponding to the $CsPbBr_3$ NP core, excitation peaks from polyfluorene ligands were observed, indicating energy transfer from the polymer ligands to the $CsPbBr_3$ NPs. Such exciton energy transfer could be beneficial when these NPs are incorporated in an emissive layer of LED devices, which requires efficient transport of electrons and holes to the NPs.

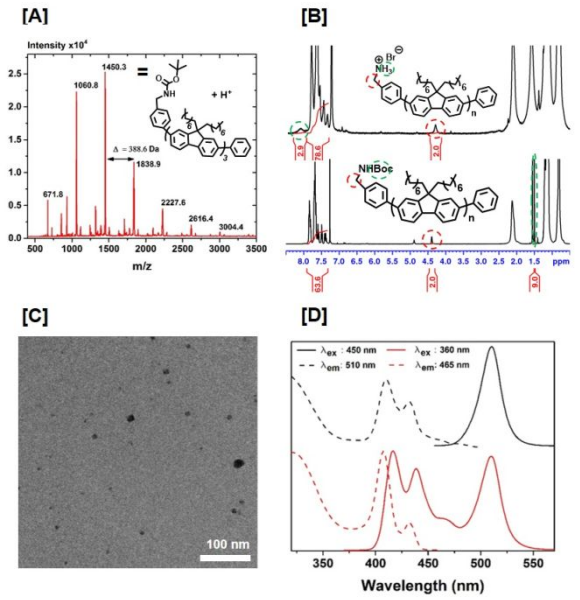

Figure 3. (A) Matrix assisted laser desorption ionization time of flight (MALDI-TOF) spectrum of PF-NHBoc; (B) ^{1}H NMR spectra of PF-NHBoc (bottom) and PF-NH_3Br (top) polymer ligands; (C) TEM image of PF-NH_3Br NPs; (D) Photoluminescence excitation (PLE, dotted) and PL (solid) spectra of the PF-NH_3Br NPs in toluene.

In summary, $CsPbBr_3$ perovskite NPs were synthesized using ammonium bromide-terminated polymers as both bromine precursors and passivating ligands. The polymer-stabilized $CsPbBr_3$ NPs were precipitated and purified in a non-polar medium without significant PL reduction, in contrast to conventional perovskite NPs stabilized by small molecule ligands. In addition, polymer-passivated NPs improved the optical clarity of the nanocomposite film, along with NP dispersion and stability, all key features that point towards applications in light-converting devices. This synthetic strategy was extended further to successfully synthesize NPs with conjugated PF-NH_3Br polymer ligands, which hold promise for applications in optoelectronics.

Conflicts of interest

There are no conflicts to declare.

Acknowledgement

Funding for this work was provided by the National Science Foundation (NSF-CHE 1506839, for materials synthesis and characterization), the Nanotechnology Consortium of the Center for UMass/Industry Research on Polymers (CUMIRP), and the Department of Energy, Basic Energy Sciences through grant DE-SC0016208 (for morphological and optical characterization).

References

1. M. A. Green, A. Ho-Baillie and H. J. Snaith, *Nat Photon*, 2014, **8**, 506-514.
2. T. M. Brenner, D. A. Egger, L. Kronik, G. Hodes and D. Cahen, *Nature Reviews Materials*, 2016, **1**, 15007.
3. S. D. Stranks, G. E. Eperon, G. Grancini, C. Menelaou, M. J. P. Alcocer, T. Leijtens, L. M. Herz, A. Petrozza and H. J. Snaith, *Science*, 2013, **342**, 341-344.
4. G. Xing, N. Mathews, S. Sun, S. S. Lim, Y. M. Lam, M. Grätzel, S. Mhaisalkar and T. C. Sum, *Science*, 2013, **342**, 344-347.
5. W. S. Yang, J. H. Noh, N. J. Jeon, Y. C. Kim, S. Ryu, J. Seo and S. I. Seok, *Science*, 2015, **348**, 1234-1237.
6. H. Cho, S.-H. Jeong, M.-H. Park, Y.-H. Kim, C. Wolf, C.-L. Lee, J. H. Heo, A. Sadhanala, N. Myoung, S. Yoo, S. H. Im, R. H. Friend and T.-W. Lee, *Science*, 2015, **350**, 1222-1225.
7. G. Xing, N. Mathews, S. S. Lim, N. Yantara, X. Liu, D. Sabba, M. Grätzel, S. Mhaisalkar and T. C. Sum, *Nat Mater*, 2014, **13**, 476-480.
8. G. Walters, B. R. Sutherland, S. Hoogland, D. Shi, R. Comin, D. P. Sellan, O. M. Bakr and E. H. Sargent, *ACS Nano*, 2015, **9**, 9340-9346.
9. L. C. Schmidt, A. Pertegás, S. González-Carrero, O. Malinkiewicz, S. Agouram, G. Mínguez Espallargas, H. J. Bolink, R. E. Galian and J. Pérez-Prieto, *Journal of the American Chemical Society*, 2014, **136**, 850-853.
10. L. Protesescu, S. Yakunin, M. I. Bodnarchuk, F. Krieg, R. Caputo, C. H. Hendon, R. X. Yang, A. Walsh and M. V. Kovalenko, *Nano Letters*, 2015, **15**, 3692-3696.
11. H. Huang, M. I. Bodnarchuk, S. V. Kershaw, M. V. Kovalenko and A. L. Rogach, *ACS Energy Letters*, 2017, **2**, 2071-2083.
12. A. Swarnkar, R. Chulliyil, V. K. Ravi, M. Irfanullah, A. Chowdhury and A. Nag, *Angewandte Chemie*, 2015, **127**, 15644-15648.
13. I. C. Smith, E. T. Hoke, D. Solis-Ibarra, M. D. McGehee and H. I. Karunadasa, *Angewandte Chemie*, 2014, **126**, 11414-11417.
14. S. Huang, Z. Li, L. Kong, N. Zhu, A. Shan and L. Li, *Journal of the American Chemical Society*, 2016, **138**, 5749-5752.
15. J. De Roo, M. Ibáñez, P. Geiregat, G. Nedelcu, W. Walravens, J. Maes, J. C. Martins, I. Van Driessche, M. V. Kovalenko and Z. Hens, *ACS Nano*, 2016, DOI: 10.1021/acsnano.5b06295.
16. M. Meyns, M. Perálvarez, A. Heuer-Jungemann, W. Hertog, M. Ibáñez, R. Nafria, A. Genç, J. Arbiol, M. V. Kovalenko, J. Carreras, A. Cabot and A. G. Kanaras, *ACS Applied Materials & Interfaces*, 2016, **8**, 19579-19586.
17. S. N. Raja, Y. Bekenstein, M. A. Koc, S. Fischer, D. Zhang, L. Lin, R. O. Ritchie, P. Yang and A. P. Alivisatos, *ACS Applied Materials & Interfaces*, 2016, **8**, 35523-35533.
18. S. Hou, Y. Guo, Y. Tang and Q. Quan, *ACS Applied Materials & Interfaces*, 2017, **9**, 18417-18422.
19. J. Xia and K. Matyjaszewski, *Macromolecules*, 1997, **30**, 7697-7700.
20. S. Aharon and L. Etgar, *Nano Letters*, 2016, **16**, 3230-3235.
21. S. A. Veldhuis, P. P. Boix, N. Yantara, M. Li, T. C. Sum, N. Mathews and S. G. Mhaisalkar, *Advanced Materials*, 2016, **28**, 6804–6834.
22. J. De Roo, M. Ibáñez, P. Geiregat, G. Nedelcu, W. Walravens, J. Maes, J. C. Martins, I. Van Driessche, M. V. Kovalenko and Z. Hens, *ACS Nano*, 2016, **10**, 2071-2081.
23. E. Jang, S. Jun, H. Jang, J. Lim, B. Kim and Y. Kim, *Advanced Materials*, 2010, **22**, 3076-3080.
24. M. E. Mackay, A. Tuteja, P. M. Duxbury, C. J. Hawker, B. Van Horn, Z. Guan, G. Chen and R. S. Krishnan, *Science*, 2006, **311**, 1740-1743.
25. D. Sunday, J. Ilavsky and D. L. Green, *Macromolecules*, 2012, **45**, 4007-4011.

[TOC]

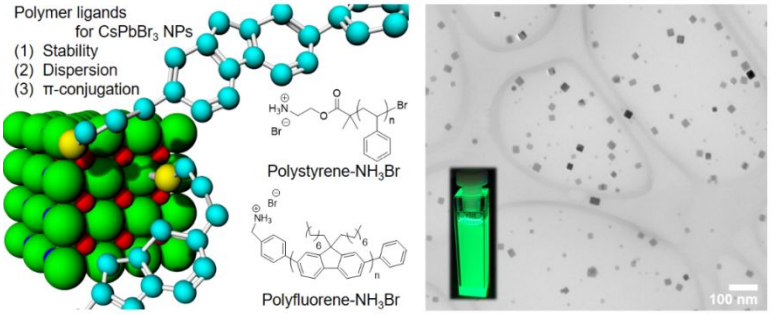

[Highlight]

Functional polymer ligands are used to prepare perovskite nanoparticles that disperse in polymer matrices.